

Boundary Element Analysis of Curved Cracked Panels with Mechanically Fastened Repair Patches

P. H. Wen¹, M. H. Aliabadi¹, A. Young²

Abstract: In this paper, applications of the boundary element method to damaged and undamaged aircraft curved panels with mechanical repairs are presented. The effects of fastened repairs are replaced by uniform distribution forces in the area of cross-section of the rivet and can be determined from the compatibility condition of displacements. A coupled boundary integral formulation of a shear deformable plate and two dimensional plane stress elasticity is used to determine the bending and membrane forces on the rivets. Domain integrals in each integral equation are determined using the dual reciprocity method. The stress intensity factors due to bending and membrane loads are evaluated by opening displacements near the crack tips. Several numerical examples are presented to demonstrate the accuracy of the proposed method. It is shown that the bending behavior and plate curvature have significant influence on the magnitude of the stress intensity factors.

keyword: Fracture, fastened repair, boundary element method, shell, stress intensity factor.

Notation

| | |
|--|--|
| a | half-length of central crack or length of edge crack |
| $c_{\alpha\beta}^K, c_{ik}^V$ | jump terms |
| D_m | number of rivets on the patch m |
| E | Young's modulus |
| $\bar{F}_{\beta}^{ml}, F_{\beta}^{ml}$ | concentrated forces in rivets |
| $\bar{f}_{\beta}^m, f_{\beta}^m$ | applied body forces for plate and patches |
| H | height of plate |
| h, h_m | thickness of plate and patches |

| | |
|--|---|
| $K_k^{bend}, K_{\beta}^{mem}$ | bending and membrane stress intensity factors |
| K_I, K_{II}, K_{III} | stress intensity factors along thickness |
| $k_{\alpha\beta}$ | curvatures |
| $\mathbf{H}, \mathbf{G}, \mathbf{D}$ | coefficient matrices of BEM |
| L | number of nodes on the boundary or number of rivets in the domain |
| $M_{\alpha\beta}, Q_{\alpha}$ | components of moment and shear for bending |
| $N_{\alpha\beta}$ | components of membrane forces |
| N_0 | applied tension load |
| p | fastener's pitch |
| p_k | traction on the boundary for bending |
| $\bar{Q}_{\beta}^{ml}, Q_{\beta}^{ml}$ | concentrated forces in rivets |
| \bar{q}_k^m, q_k^m | applied body forces for plate and patches |
| q_0 | uniform pressure load |
| $T_{\alpha\beta}$ | fundamental solution of traction |
| t_{β} | traction on the boundary for two dimensions |
| $U_{\alpha\beta}$ | fundamental solution of displacement |
| u_{α} | displacements of two dimension elasticity |
| x_k | coordinate system |
| \mathbf{x} | collocation point on the boundary |
| \mathbf{X} | domain point |
| W | width of plate |
| w_k | rotations and deflection of plate bending |
| Γ | boundary of plate |
| Ω | domains |
| Φ | diameter of rivet |
| Φ^K, Φ^V | coefficients of rivet |
| $\Delta u_{\alpha}, \Delta w_k$ | discontinuities of displacements on crack surface |
| σ_0 | uniform tension |
| ν | Poisson's ratio |

¹ Department of Engineering, Queen Mary and Westfield College, London University, London, E1 4NS, UK

² Structural Materials Centre, DERA, Farnborough, Hants, GU14 6TD, UK

1 Introduction

Mechanically fastened repair patches are efficient design solutions for repair of damage panels in aircraft structures, as the stress intensity factors at crack tips can be reduced, and hence, fatigue life increased. There is growing use of adhesive bonding, however mechanical fasteners such as rivets and bolts remain the most common technique for attaching patches to structures. Mechanically fastened joints are the recommended repair methods for heavily loaded components while adhesive bonding is preferred for the repair of lightly loaded components.

It is generally difficult to analyse cracked panels with mechanically fastened repairs by the finite element method due to the necessity of modelling the rivet and the interaction between the panel and rivet. Analysis by the finite element method (FEM) of the bending effect was carried out by Chu and Lin (1993) for a composite sheet and patch. They reported a reduction in the efficiency of the patching with increasing out-of-plane deflection of the plate. The analysis of crack in aging aircraft structures and composite patch repairs can be found in [Park, Ogiso, Atluri (1992); Chow, Atluri (1997)] The bending behavior can be found in lap joints structures; this was comprehensively studied by Fawaz (1997) by the finite element method using three dimension modelling. The boundary element method (BEM) is now an established method for analysing fracture mechanics problems [see Aliabadi (1998)]. The application of the boundary element method to mechanically fastened repairs and lap joints has been reported by Salgado and Aliabadi (1997) using a two-dimensional formulation.

In this paper, BEM is applied to curved panels with mechanically fastened repair patches and the coupled effect of the membrane and out-of-plane bending forces are considered by using Reissner's plate and two dimensional stress plane theories. The influence of attachments on a sheet are replaced by the distribution of body forces which include two body forces in the plane, two moments body forces and one out-of-plane force through the cross-section of the rivets. Coupled boundary integral equations are established for the analysis of curved panels and domain integrals in each equation are transferred to boundary integrals using the dual reciprocity method. A comparison was made with the results obtained by the finite element method.

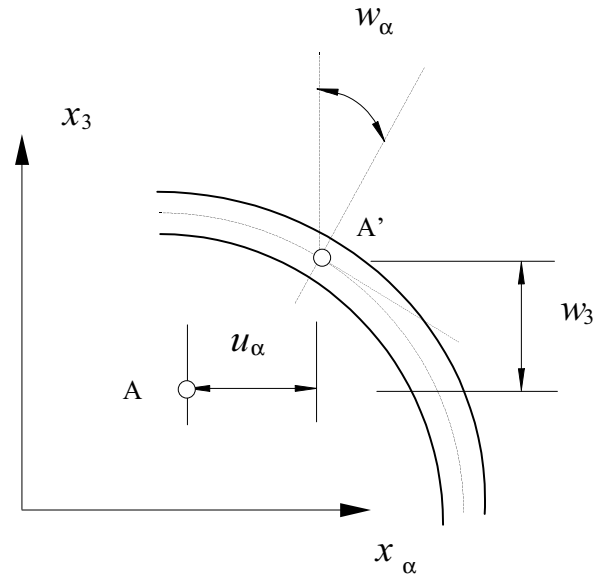


Figure 1 : Coordinate system.

2 Boundary integral equations for a shallow shell

Consider a shallow shell with a quadratic middle surface given by

$$z = -\frac{1}{2}(k_{11}x_1^2 + k_{22}x_2^2) \quad (1)$$

where z denotes the position of middle surface of the shell, k_{11} and k_{22} are the principal curvatures of the shell in the x_1 and x_2 directions respectively (see Figure 1). The elasticity relations between stresses and displacements are given by Shi and Hagendorf (1997).

$$\begin{aligned} N_{\alpha\beta} &= \frac{1-\nu}{2}B \left(u_{\alpha,\beta} + u_{\beta,\alpha} + \frac{2\nu}{1-\nu}u_{\gamma,\gamma}\delta_{\alpha,\beta} \right) \\ &\quad + B[(1-\nu)k_{\alpha\beta} + \nu k_{\phi\phi}\delta_{\alpha\beta}]w_3 \\ Q_\alpha &= \frac{1-\nu}{2}D\lambda^2(w_\alpha + w_{3,\alpha}) \\ M_{\alpha\beta} &= \frac{1-\nu}{2}D \left(w_{\alpha,\beta} + w_{\beta,\alpha} + \frac{2\nu}{1-\nu}w_{\gamma,\gamma}\delta_{\alpha,\beta} \right) \end{aligned} \quad (2)$$

where $N_{\alpha\beta}(\alpha, \beta = 1, 2)$ denotes the stress resultants for two dimensional plane stress elasticity, $M_{\alpha\beta}$ and Q_α are the bending moment and shear force stress resultants for plate bending problems, u_β and $w_k(k = 1, 2, 3)$ represent displacements, rotation ($k = 1, 2$) and deflection

($k = 3$) [see definitions Wen, Aliabadi, Young (1999)]. $B = Eh/(1 - \nu^2)$ is tension stiffness; $D = Eh^3/12(1 - \nu^2)$ is bending stiffness of the shell; $\lambda = \sqrt{10}/h$ is the plate factor and h is the thickness of the shell; E and ν are the elastic constants.

The boundary integral equations for the shallow shell problem can be written as [Wen, Aliabadi, Young (2000)]

$$\begin{aligned} & c_{\alpha\beta}^k(\mathbf{x}')u_\beta(\mathbf{x}') + \int_{\Gamma} -T_{\alpha\beta}^k(\mathbf{x}', \mathbf{x})u_\beta(\mathbf{x})d\Gamma - \int_{\Gamma} U_{\alpha\beta}^k(\mathbf{x}', \mathbf{x})t_\beta(\mathbf{x})d\Gamma \\ & + B[(1 - \nu)k_{\beta\gamma} + \nu k_{\phi\phi}\delta_{\beta\gamma}] \int_{\Gamma} U_{\alpha\gamma}^k(\mathbf{x}', \mathbf{x})n_\beta(\mathbf{x})w_3(\mathbf{x})d\Gamma \\ & - B[(1 - \nu)k_{\beta\gamma} + \nu k_{\phi\phi}\delta_{\beta\gamma}] \int_{\Omega} U_{\alpha\beta}^k(\mathbf{x}', \mathbf{X})w_{3,\gamma}(\mathbf{X})d\Omega \\ & = \int_{\Omega} U_{\alpha\beta}^k(\mathbf{x}', \mathbf{X})\bar{f}_\beta(\mathbf{X})d\Omega \end{aligned} \quad (3)$$

where \int denotes a Cauchy principal-value integral, $\mathbf{x} \in \Gamma$ and $\mathbf{X} \in \Omega$ are the field points and $t_\beta = N_{\alpha\beta}n_\alpha$, n_α denotes the component of the outward to the boundary, \bar{f}_β represents the body forces, $\mathbf{x}' \in \Omega$ is the source point. $c_{\alpha\beta}^k(\mathbf{x}')$ is a function of the geometry variation at the boundary point, which can be determined by rigid body movements. $U_{\alpha\beta}^k$ and $T_{\alpha\beta}^k$ are displacement and traction fundamental solutions respectively for the plane stress problem [see for example Aliabadi (1998)]. For plate bending, the boundary integral equation can be written as in Wen, Aliabadi and Young (1999)

$$\begin{aligned} & c_{ik}^v(\mathbf{x}')w_k(\mathbf{x}') + \int_{\Gamma} -T_{ik}^v(\mathbf{x}', \mathbf{x})w_k(\mathbf{x})d\Gamma - \int_{\Gamma} U_{ik}^v(\mathbf{x}', \mathbf{x})p_k(\mathbf{x})d\Gamma \\ & + B[(1 - \nu)k_{\alpha\beta} + \nu k_{\phi\phi}\delta_{\alpha\beta}] \int_{\Omega} U_{i3}^v(\mathbf{x}', \mathbf{X})u_{\alpha,\beta}(\mathbf{X})d\Omega \quad (4) \\ & - B(k_{11}^2 + k_{22}^2 + 2\nu k_{11}k_{22}) \int_{\Omega} U_{i3}^v(\mathbf{x}', \mathbf{X})w_3(\mathbf{X})d\Omega \\ & = \int_{\Omega} U_{ik}^v(\mathbf{x}', \mathbf{X})\bar{q}_k(\mathbf{X})d\Omega \end{aligned}$$

where $p_\beta = M_{\alpha\beta}n_\alpha$, $p_3 = Q_\alpha n_\alpha$ and $c_{\alpha\beta}^v(\mathbf{x}')$ is a function of the geometry variation at the boundary point, and \bar{q}_k are the body forces. U_{ij}^v and T_{ij}^v are displacement and traction fundamental solutions respectively for the plate bending problem given by Vander (1982).

For the dual boundary element method, the traction boundary integral equations are applied on the crack surface \mathbf{x}'^+ and can be obtained as follows:

$$\frac{1}{2}[t_\alpha(\mathbf{x}'^+) - t_\alpha(\mathbf{x}'^-)] = n_\beta(\mathbf{x}'^+) \int_{\Gamma} U_{\alpha\beta\gamma}^k(\mathbf{x}'^+, \mathbf{x})t_\gamma(\mathbf{x})d\Gamma$$

$$\begin{aligned} & -n_\beta(\mathbf{x}'^+) \int_{\Gamma} T_{\alpha\beta\gamma}^k(\mathbf{x}'^+, \mathbf{x})u_\gamma(\mathbf{x})d\Gamma \\ & -n_\beta(\mathbf{x}'^+)B[(1 - \nu)k_{\theta\gamma} + \nu k_{\phi\phi}\delta_{\theta\gamma}] \int_{\Gamma} U_{\alpha\beta\gamma}^k(\mathbf{x}'^+, \mathbf{x})n_\theta(\mathbf{x})w_3(\mathbf{x})d\Gamma \\ & +n_\beta(\mathbf{x}'^+)B[(1 - \nu)k_{\theta\gamma} + \nu k_{\phi\phi}\delta_{\theta\gamma}] \int_{\Omega} U_{\alpha\beta\gamma}^k(\mathbf{x}'^+, \mathbf{X})w_{3,\theta}(\mathbf{X})d\Omega \\ & +n_\beta(\mathbf{x}'^+) \int_{\Omega} U_{\alpha\beta\gamma}^k(\mathbf{x}'^+, \mathbf{X})\bar{f}_\gamma(\mathbf{X})d\Omega \end{aligned} \quad (5)$$

for in-plane stress, where \int denotes a Hadamard principal-value integral, and

$$\begin{aligned} & \frac{1}{2}[p_i(\mathbf{x}'^+) - p_i(\mathbf{x}'^-)] = n_\beta(\mathbf{x}'^+) \int_{\Gamma} U_{i\beta k}^p(\mathbf{x}'^+, \mathbf{x})p_k(\mathbf{x})d\Gamma \\ & -n_\beta(\mathbf{x}'^+) \int_{\Gamma} T_{i\beta k}^v(\mathbf{x}'^+, \mathbf{x})w_k(\mathbf{x})d\Gamma \\ & -n_\beta(\mathbf{x}'^+)B[(1 - \nu)k_{\gamma\theta} + \nu k_{\phi\phi}\delta_{\gamma\theta}] \int_{\Omega} U_{i\beta 3}^v(\mathbf{x}'^+, \mathbf{X})u_{\gamma,\theta}d\Omega \\ & +n_\beta(\mathbf{x}'^+)B(k_{11}^2 + k_{22}^2 + 2\nu k_{11}k_{22}) \int_{\Omega} U_{i\beta 3}^v(\mathbf{x}'^+, \mathbf{X})w_3d\Omega \\ & +n_\beta(\mathbf{x}'^+) \int_{\Omega} U_{i\beta k}^v(\mathbf{x}'^+, \mathbf{X})\bar{q}_k(\mathbf{X})d\Omega \end{aligned} \quad (6)$$

for plate bending. Consider the properties of fundamental solution as

$$U_{\alpha\beta}(\mathbf{x}'^+, \mathbf{x}) = U_{\alpha\beta}(\mathbf{x}'^-, \mathbf{x}), U_{\alpha\beta\gamma}(\mathbf{x}'^+, \mathbf{x}) = U_{\alpha\beta\gamma}(\mathbf{x}'^-, \mathbf{x})$$

and

$$T_{\alpha\beta}(\mathbf{x}'^+, \mathbf{x}) = -T_{\alpha\beta}(\mathbf{x}'^-, \mathbf{x}), T_{\alpha\beta\gamma}(\mathbf{x}'^+, \mathbf{x}) = -T_{\alpha\beta\gamma}(\mathbf{x}'^-, \mathbf{x})$$

The boundary displacement integral equations (1) and (8) can be rewritten, if $t_\beta^+ + t_\beta^- = 0$ for two dimensions and $p_i^+ + p_i^- = 0$, as

$$\begin{aligned} & c_{\alpha\beta}^k(\mathbf{x}')u_\beta(\mathbf{x}') + \int_{\Gamma_0} T_{\alpha\beta}^k(\mathbf{x}', \mathbf{x})u_\beta(\mathbf{x})d\Gamma \\ & + \int_{C^+} T_{\alpha\beta}^k(\mathbf{x}', \mathbf{x}^+)\Delta u_\beta d\Gamma - \int_{\Gamma_0} U_{\alpha\beta}^k(\mathbf{x}', \mathbf{x})t_\beta(\mathbf{x})d\Gamma \\ & + B[(1 - \nu)k_{\beta\gamma} + \nu k_{\phi\phi}\delta_{\beta\gamma}] \left(\int_{\Gamma_0} U_{\alpha\gamma}^k(\mathbf{x}', \mathbf{x})n_\beta(\mathbf{x})w_3d\Gamma \right. \\ & \left. + \int_{C^+} U_{\alpha\gamma}^k(\mathbf{x}', \mathbf{x})n_\beta(\mathbf{x})\Delta w_3(\mathbf{x})d\Gamma \right) \\ & - B \int_{\Omega} U_{\alpha\beta}^k(\mathbf{x}', \mathbf{X})[(1 - \nu)k_{\beta\gamma} + \nu k_{\phi\phi}\delta_{\beta\gamma}]w_{3,\gamma}(\mathbf{X})d\Omega \\ & = \int_{\Omega} U_{\alpha\beta}^k(\mathbf{x}', \mathbf{X})\bar{f}_\beta d\Omega \end{aligned} \quad (7)$$

and

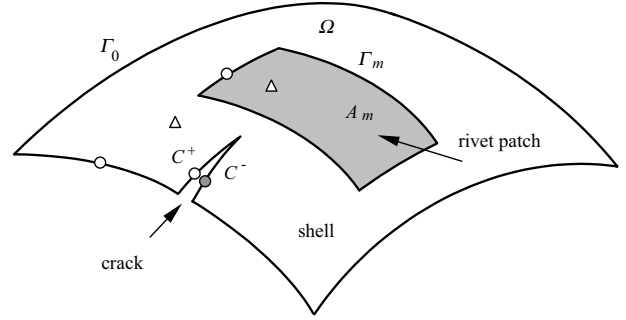
$$\begin{aligned}
& c_{ik}^v(\mathbf{x}') w_k(\mathbf{x}') + \int_{\Gamma_0} T_{ik}^v(\mathbf{x}', \mathbf{x}) w_k(\mathbf{x}) d\Gamma \\
& + \int_{C^+} T_{ik}^v(\mathbf{x}', \mathbf{x}^+) \Delta w_k d\Gamma - \int_{\Gamma_0} U_{ik}^v(\mathbf{x}', \mathbf{x}) p_k(\mathbf{x}) d\Gamma(\mathbf{x}) \\
& + B[(1-\nu)k_{\alpha\beta} + \nu k_{\phi\phi} \delta_{\alpha\beta}] \int_{\Omega} U_{i3}^v(\mathbf{x}', \mathbf{X}) u_{\alpha,\beta} d\Omega \\
& - B(k_{11}^2 + k_{22}^2 + 2\nu k_{11} k_{22}) \int_{\Omega} U_{i3}^v(\mathbf{x}', \mathbf{X}) w_3 d\Omega \\
& = \int_{\Omega} U_{ik}^v(\mathbf{x}', \mathbf{X}) \bar{q}_k d\Omega
\end{aligned} \tag{8}$$

and the traction equations

$$\begin{aligned}
& \frac{1}{2} t_{\alpha}(\mathbf{x}^+) - \frac{1}{2} t_{\alpha}(\mathbf{x}^-) = n_{\beta} \int_{\Gamma_0} U_{\alpha\beta\gamma}^K(\mathbf{x}^+, \mathbf{x}) t_{\gamma}(\mathbf{x}) d\Gamma \\
& - n_{\beta}(\mathbf{x}'^+) \int_{\Gamma_0} T_{\alpha\beta\gamma}^K(\mathbf{x}'^+, \mathbf{x}) u_{\gamma}(\mathbf{x}) d\Gamma - n_{\beta}(\mathbf{x}'^+) \\
& \int_{C^+} T_{\alpha\beta\gamma}^K(\mathbf{x}'^+, \mathbf{x}^+) \Delta u_{\gamma} d\Gamma \\
& - n_{\beta} B[(1-\nu)k_{\theta\gamma} + \nu k_{\phi\phi} \delta_{\theta\gamma}] \left(\int_{\Gamma_0} U_{\alpha\beta\gamma}^K(\mathbf{x}^+, \mathbf{x}) n_{\theta}(\mathbf{x}) w_3 d\Gamma \right. \\
& \left. + \int_{C^+} U_{\alpha\beta\gamma}^K(\mathbf{x}^+, \mathbf{x}) n_{\theta}(\mathbf{x}) \Delta w_3 d\Gamma \right) \\
& + n_{\beta} B \int_{\Omega} U_{\alpha\beta\gamma}^K(\mathbf{x}^+, \mathbf{X}) [(1-\nu)k_{\theta\gamma} + \nu k_{\phi\phi} \delta_{\theta\gamma}] w_{3,\theta}(\mathbf{X}) d\Omega \\
& + n_{\beta} \int_{\Omega} U_{\alpha\beta\gamma}^K(\mathbf{x}^+, \mathbf{X}) \bar{f}_{\gamma} d\Omega
\end{aligned} \tag{9}$$

and

$$\begin{aligned}
& \frac{1}{2} p_i(\mathbf{x}^+) - \frac{1}{2} p_i(\mathbf{x}^-) = n_{\beta} \int_{\Gamma_0} U_{i\beta k}^v(\mathbf{X}^+, \mathbf{x}) p_k(\mathbf{x}) d\Gamma \\
& - n_{\beta} \int_{\Gamma_0} T_{i\beta k}^v(\mathbf{X}^+, \mathbf{x}) w_k(\mathbf{x}) d\Gamma \\
& - n_{\beta}(\mathbf{x}'^+) \int_{C^+} T_{i\beta k}^v(\mathbf{x}'^+, \mathbf{x}^+) \Delta w_k d\Gamma \\
& - n_{\beta} B[(1-\nu)k_{\gamma\theta} + \nu k_{\phi\phi} \delta_{\gamma\theta}] \int_{\Omega} U_{i\beta 3}^v(\mathbf{x}^+, \mathbf{X}) u_{\gamma,\theta} d\Omega \\
& - n_{\beta} B(k_{11}^2 + k_{22}^2 + 2\nu k_{11} k_{22}) \int_{\Omega} U_{i\beta 3}^v(\mathbf{x}^+, \mathbf{X}) w_3 d\Omega \\
& - n_{\beta} B[(1-\nu)k_{\gamma\theta} + \nu k_{\phi\phi} \delta_{\gamma\theta}] \int_{\Omega} U_{i\beta 3}^v(\mathbf{x}^+, \mathbf{X}) u_{\gamma,\theta} d\Omega
\end{aligned}$$



- △ Domain collocation points, Equations (3) and (4)
- Boundary and one of the crack surfaces, Equations (3) and (4)
- One of the crack surfaces, Equations (5) and (6)

Figure 2 : Strategy of the dual boundary element method

$$\begin{aligned}
& -n_{\beta} B(k_{11}^2 + k_{22}^2 + 2\nu k_{11} k_{22}) \int_{\Omega} U_{i\beta 3}^v(\mathbf{x}^+, \mathbf{X}) w_3 d\Omega \\
& + n_{\beta} \int_{\Omega} U_{i\beta k}^v(\mathbf{x}^+, \mathbf{X}) \bar{q}_k d\Omega
\end{aligned} \tag{10}$$

where $\Gamma_0 = \Gamma - C^+ - C^-$ is the boundary, excluding crack surfaces, C^+ and C^- represent the upper and lower crack surfaces and Δu_{β} and Δw_k are the discontinuities of displacements and defined as $\Delta u_{\beta} = u_{\beta}^+ - u_{\beta}^-$ and $\Delta w_k = w_k^+ - w_k^-$. In this case, the unknowns can be reduced to the displacements or traction on the boundary Γ_0 and the discontinuity of displacement on the crack surface C . Applying the displacement integral equation on the boundary Γ_0 and the traction equation on the crack surface C^+ gives a linear system to determine all unknowns, including the discontinuity displacements on the crack surface Δu_{β} and Δw_k . The strategy of DBEM is illustrated in Figure 2.

3 Evaluation of domain integrals

Let $\bar{F}_{\alpha}^{mn}(\mathbf{X}^n)$ and $\bar{Q}_k^{mn}(\mathbf{X}^n)$ represent the five concentrate forces on the middle plane of the sheet in the area of attachment m , with rivet geometry central point \mathbf{X}^n and $A_m (= \pi\phi^2/4)$ denoting the section area of the rivets on the m th patch (see Figure 3), ϕ denotes the diameter of the rivet, thus

$$\bar{f}_{\alpha}^m(\mathbf{X}) = \bar{f}_{\alpha}^0 + \frac{\bar{F}_k^{mn}(\mathbf{X}^n)}{A_m},$$

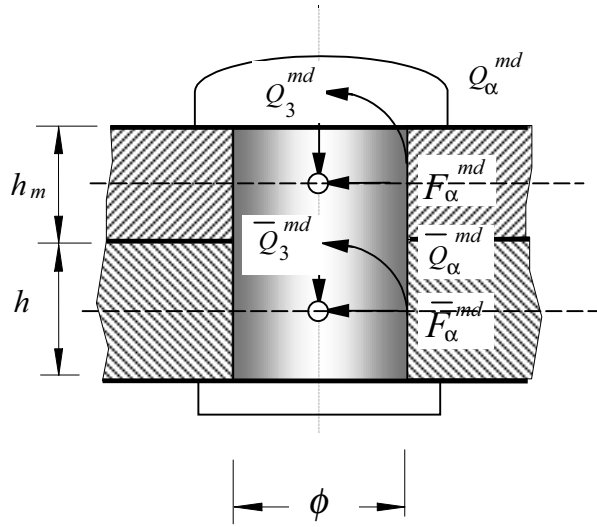


Figure 3 : Rivet and interaction forces.

$$\bar{q}_k^{mn}(\mathbf{X}) = \bar{q}_k^0 + \frac{\bar{Q}_k^{mn}(\mathbf{X}^n)}{A_m} \mathbf{X} \in A_m$$

where $\bar{f}_\alpha^0, \bar{q}_k^0$ are applied body forces in the domain Ω . Domain integrals containing \bar{f}_β and \bar{q}_k in equations (3)-(6) can be evaluated in the way shown in Wen, Aliabadi and Young (2000). In the boundary integral equations, (3)-(6), there are eight domain integrals if body forces for two-dimensional and bending problems are $\bar{f}_\alpha^0 = 0, \bar{q}_\alpha^0 = 0$ ($\alpha = 1, 2$) and $\bar{q}_3^0 = q$, as follows:

$$\begin{aligned} I_i^{(1)} &= \int_{\Omega} U_{i3}^V w_3 d\Omega, \quad I_{i\alpha\beta}^{(2)} = \int_{\Omega} U_{i3}^V \frac{\partial u_\alpha}{\partial x_\beta} d\Omega, \\ I_i^{(3)} &= \int_{\Omega} U_{i3}^V q d\Omega, \quad I_{\alpha\beta\gamma}^{(4)} = \int_{\Omega} U_{\alpha\beta}^K \frac{\partial w_3}{\partial x_\gamma} d\Omega, \\ I_i^{(5)} &= n_\beta \int_{\Omega} U_{i\beta 3}^V w_3 d\Omega, \quad I_{i\gamma\theta}^{(6)} = n_\beta \int_{\Omega} U_{i\beta 3}^V \frac{\partial u_\gamma}{\partial x_\theta} d\Omega \\ I_i^{(7)} &= n_\beta \int_{\Omega} U_{i\beta 3}^V q d\Omega, \quad I_{\alpha\gamma\theta}^{(8)} = n_\beta \int_{\Omega} U_{\alpha\beta\gamma}^K \frac{\partial w_3}{\partial x_\theta} d\Omega. \end{aligned} \quad (11)$$

All of above domain integrals can be transformed into boundary integrals Using of dual reciprocity method [see Wen, Aliabadi, Young (2000) for details].

4 Numerical implementation

4.1 Analysis of rivet

Consider the equilibrium of fasteners. Suppose there are M patches on the repaired shell, therefore there should be

$5 \sum_{m=1}^M L_m^d$ equations related to the concentrated forces on rivet \mathbf{X}^n :

$$\begin{aligned} \bar{F}_\alpha^{mn} + F_\alpha^{mn} &= 0, \\ \bar{Q}_3^{mn} + Q_3^{mn} &= 0 \\ \bar{Q}_\alpha^{mn} + Q_\alpha^{mn} \pm \frac{h+h_m}{2} F_\alpha^{mn} &= 0 \end{aligned} \quad (12)$$

$n = 1, 2, \dots, N_m; \quad m = 1, 2, \dots, M$

for $\alpha = 1, 2$, where N_m represents the number of rivets on the m th patch. The displacements, rotations and deflections on the rivets \mathbf{X}^n at the sheet and a corresponding point at patch m are compatible with the shear deformation of the rivets. Therefore M sets of connection conditions can be derived:

$$u_\alpha^n - u_\alpha^{mn} = \Phi^\kappa \bar{F}_\alpha^{mn} \pm \frac{h+h_m}{2} w_\alpha^n; \quad \alpha = 1, 2 \quad (13)$$

$$w_k^n - w_k^{mn} = \Phi^V \bar{Q}_k^{mn} \quad k = 1, 2, 3 \quad (14)$$

where u_α^n, w_k^n are the displacements of the sheet on rivet \mathbf{X}^n , u_α^{mn}, w_k^{mn} are the displacement of the m th patch, \bar{F}_α^{mn} and \bar{Q}_k^{mn} represent the body forces in the section area A_m of rivets on the m th patch. For the patches on the top surface of the sheet, the + sign is selected. Φ^κ is defined as the coefficient of shear deformation of the fasteners used to connect the sheet and the patch and can be determined from the empirical equation derived by Swift (1974):

$$\Phi^\kappa = \frac{1}{E_R \Phi} \{a_0 + a_1 \Phi [\frac{1}{h} + \frac{1}{h_m}]\} \quad (15)$$

where E_R is the Young's modulus of the rivets, h and h_m denote the thicknesses of sheet and the m th patch respectively. The constants a_0 and a_1 are chosen as 5.0 and 0.8 respectively to correspond to aluminium rivets [Swift (1974)]. Φ^V are the coefficients of bending and axial deformation of rivet and in the following analysis they are ignored, i.e. $\Phi^V = 0$.

4.2 Discretization of integral equations

The displacement boundary integral equation for repaired shell can be re-arranged, in terms of rivet forces, as

$$\begin{aligned} c_{\alpha\beta}^K(\mathbf{x}') u_\beta(\mathbf{x}') + \int_{\Gamma} T_{\alpha\beta}^K(\mathbf{x}', \mathbf{x}) u_\beta(\mathbf{x}) d\Gamma \\ - \int_{\Gamma} U_{\alpha\beta}^K(\mathbf{x}', \mathbf{x}) t_\beta(\mathbf{x}) d\Gamma \end{aligned}$$

$$\begin{aligned}
& +B[(1-\nu)k_{\beta\gamma} + \nu k_{\phi\phi}\delta_{\beta\gamma}] \int_{\Gamma} U_{\alpha\gamma}^K(\mathbf{x}', \mathbf{x}) n_{\beta}(\mathbf{x}) w_3(\mathbf{x}) d\Gamma \\
& -B[(1-\nu)k_{\beta\gamma} + \nu k_{\phi\phi}\delta_{\beta\gamma}] I_{\alpha\beta\gamma}^{(4)} \\
& = \sum_{m=1}^M \sum_{d=1}^{L_m^d} U_{\alpha\beta}^K(\mathbf{x}', \mathbf{X}_d) \bar{F}_{\beta}^{md}
\end{aligned} \quad (16)$$

and

$$\begin{aligned}
& c_{ik}^v(\mathbf{x}') w_k(\mathbf{x}') + \int_{\Gamma} T_{ik}^v(\mathbf{x}', \mathbf{x}) w_k(\mathbf{x}) d\Gamma - \int_{\Gamma} U_{ik}^v(\mathbf{x}', \mathbf{x}) p_k(\mathbf{x}) d\Gamma \\
& + B[(1-\nu)k_{\alpha\beta} + \nu k_{\phi\phi}\delta_{\alpha\beta}] I_{i\alpha\beta}^{(2)} - B(k_{11}^2 + k_{22}^2 + 2\nu k_{11}k_{22}) I_i^{(1)} \\
& = I_i^{(3)} + \frac{1}{h} \sum_{m=1}^M \sum_{d=1}^{L_m^d} U_{ik}^v(\mathbf{x}', \mathbf{X}) \bar{Q}_k^{md}
\end{aligned} \quad (17)$$

The traction integral equation on the crack surface is

$$\begin{aligned}
& \frac{1}{2} [t_{\alpha}(\mathbf{x}^{'+}) - t_{\alpha}(\mathbf{x}'^{-})] = n_{\beta}(\mathbf{x}^{'+}) \int_{\Gamma} U_{\alpha\beta\gamma}^K(\mathbf{x}^{'+}, \mathbf{x}) t_{\gamma}(\mathbf{x}) d\Gamma \\
& - n_{\beta} \int_{\Gamma} T_{\alpha\beta\gamma}^K(\mathbf{x}^{\pm}, \mathbf{x}) u_{\gamma}(\mathbf{x}) d\Gamma \\
& - n_{\beta}(\mathbf{x}^{'+}) B[(1-\nu)k_{\theta\gamma} + \nu k_{\phi\phi}\delta_{\theta\gamma}] \int_{\Gamma} U_{\alpha\beta\gamma}^K(\mathbf{x}^{'+}, \mathbf{x}) n_{\theta}(\mathbf{x}) w_3(\mathbf{x}) d\Gamma \\
& + B[(1-\nu)k_{\theta\gamma} + \nu k_{\phi\phi}\delta_{\theta\gamma}] I_{\alpha\gamma\theta}^{(8)} \\
& + n_{\beta}(\mathbf{x}^{'+}) \sum_{m=1}^M \sum_{d=1}^{L_m^d} U_{\alpha\beta\gamma}^K(\mathbf{x}^{'+}, \mathbf{X}_d) \bar{F}_{\gamma}^{md}
\end{aligned} \quad (18)$$

and

$$\begin{aligned}
& \frac{1}{2} [p_i(\mathbf{x}^{'+}) - p_i(\mathbf{x}'^{-})] = n_{\beta}(\mathbf{x}^{'+}) \int_{\Gamma} U_{i\beta k}^v(\mathbf{x}^{'+}, \mathbf{x}) p_k(\mathbf{x}) d\Gamma \\
& - n_{\beta}(\mathbf{x}^{'+}) \int_{\Gamma} T_{i\beta k}^v(\mathbf{x}^{'+}, \mathbf{x}) w_k(\mathbf{x}) d\Gamma \\
& - B[(1-\nu)k_{\gamma\theta} + \nu k_{\phi\phi}\delta_{\gamma\theta}] I_{i\gamma\theta}^{(6)} - B(k_{11}^2 + k_{22}^2 + 2\nu k_{11}k_{22}) I_i^{(5)} \\
& + I_i^{(7)} + n_{\beta}(\mathbf{x}^{'+}) \sum_{m=1}^M \sum_{d=1}^{L_m^d} U_{i\beta k}^v(\mathbf{X}', \mathbf{X}_d) \bar{Q}_k^{md}
\end{aligned} \quad (19)$$

After the collocation point passes through all the collocation nodes on the boundary (including crack surfaces) and in the domain, equations (16)-(19) give the following linear equations in matrix form:

$$\begin{Bmatrix} \mathbf{H}^K \mathbf{H}^w \\ \mathbf{H}^u \mathbf{H}^v \end{Bmatrix} \begin{Bmatrix} \mathbf{u} \\ \mathbf{w} \end{Bmatrix} = \begin{Bmatrix} \mathbf{G}^K \mathbf{0} \\ \mathbf{0} \mathbf{G}^v \end{Bmatrix} \begin{Bmatrix} \mathbf{t} \\ \mathbf{p} \end{Bmatrix} + \begin{Bmatrix} \mathbf{b}^K + \sum \mathbf{D}_m^K \bar{\mathbf{F}}_m \\ \mathbf{b}^v + \sum \mathbf{D}_m^v \bar{\mathbf{Q}}_m \end{Bmatrix} \quad (20)$$

where \mathbf{H}^K , \mathbf{H}^v , \mathbf{G}^K and \mathbf{G}^v are the standard boundary element influence matrices for plane stress elasticity and the plate bending problem respectively, \mathbf{H}^w , \mathbf{H}^u are coupling matrices caused by the shell curvatures k_{11} , k_{22} , matrices \mathbf{b}^K , \mathbf{b}^v are domain integrals caused by applied body forces, matrices \mathbf{D}_m^K , \mathbf{D}_m^v are determined by the displacement fundamental solution. Similar integral equations can be obtained for the m th patch ($m = 1, 2, \dots, M$) in the form

$$\begin{Bmatrix} \mathbf{H}^{Km} \mathbf{H}^{wm} \\ \mathbf{H}^{um} \mathbf{H}^{vm} \end{Bmatrix} \begin{Bmatrix} \mathbf{u}^m \\ \mathbf{w}^m \end{Bmatrix} = \begin{Bmatrix} \mathbf{G}^{Km} \mathbf{0} \\ \mathbf{0} \mathbf{G}^{vm} \end{Bmatrix} \begin{Bmatrix} \mathbf{t}^m \\ \mathbf{p}^m \end{Bmatrix} + \begin{Bmatrix} \mathbf{D}_m^K \mathbf{F}_m \\ \mathbf{D}_m^v \mathbf{Q}_m \end{Bmatrix} \quad (21)$$

Also the equilibrium equation and displacement compatibility equations can be arranged, in the matrix form, as

$$\begin{aligned}
& \{\bar{\mathbf{F}}_m, \bar{\mathbf{Q}}\} + \mathbf{C}_1 \{\mathbf{F}_m, \mathbf{Q}_m\} = \mathbf{0} \\
& \{\mathbf{u}, \mathbf{w}\} + \mathbf{C}_2 \mathbf{f}_m + \mathbf{C}_3 \{\mathbf{u}^m, \mathbf{w}^m\} = \mathbf{0}
\end{aligned} \quad (22)$$

where \mathbf{C}_k are constants. Suppose there are L_0 boundary element nodes on the Γ of the sheet, L_m on the boundary Γ_m and L_m^d domain points (including rivets points) in the patch area A_m , the total number of unknowns should be $5 \times (L_0 + \sum L_m) + 4 \times 5 \times \sum L_m^d$ for the sheet and patch. The number of boundary integral equations including displacement and traction equations is $5 \times (L_0 + \sum L_m) + 2 \times 5 \times \sum L_m^d$ and the number of equilibrium equations and displacement compatibility conditions in the patch area A_m should be $2 \times \sum L_m^d$. The unknowns on the boundaries of the sheet and patches, displacement in the patch areas and forces on the rivets can be obtained.

4.3 Determination of stress intensity factors

By solving the linear system (21)-(23), the displacement discontinuities Δu_{α} and Δw_k can be obtained. If the crack is parallel to x_1 the relationships between discontinuity displacements and stress intensity factors can be written as [see Dirgantara and Aliabadi (1999)]:

$$\Delta u_1 = u_1^+ - u_1^- = \frac{8\sqrt{r}}{E\sqrt{2\pi}} K_2^m$$

$$\begin{aligned}\Delta u_2 &= u_2^+ - u_2^- = \frac{8\sqrt{r}}{E\sqrt{2\pi}}K_1^m \\ \Delta w_1 &= w_1^+ - w_1^- = \frac{48\sqrt{2r}}{Eh^3}K_2^b \\ \Delta w_2 &= w_2^+ - w_2^- = \frac{48\sqrt{2r}}{Eh^3}K_1^b \\ \Delta w_3 &= w_3^+ - w_3^- = \frac{24(1+\nu)\sqrt{2r}}{5Eh}K_3^b\end{aligned}\quad (23)$$

where + and - denote the upper and lower crack surfaces, r represents the distance from the calculation point on the crack surface to the crack tip, K_1^m and K_2^m are membrane stress intensity factors and K_1^b , K_2^b and K_3^b are bending stress intensity factors. The mixed mode of stress intensity factors along the thickness of the plate are given as

$$\begin{aligned}K_I(x_3) &= K_1^m + \frac{12x_3}{h^3}K_1^b \\ K_{II}(x_3) &= K_2^m + \frac{12x_3}{h^3}K_2^b \\ K_{III}(x_3) &= \frac{3}{2h} \left[1 - \left(\frac{2x_3}{h} \right)^2 \right] K_3^b.\end{aligned}\quad (24)$$

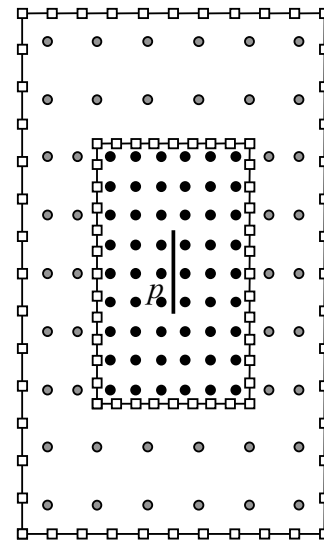
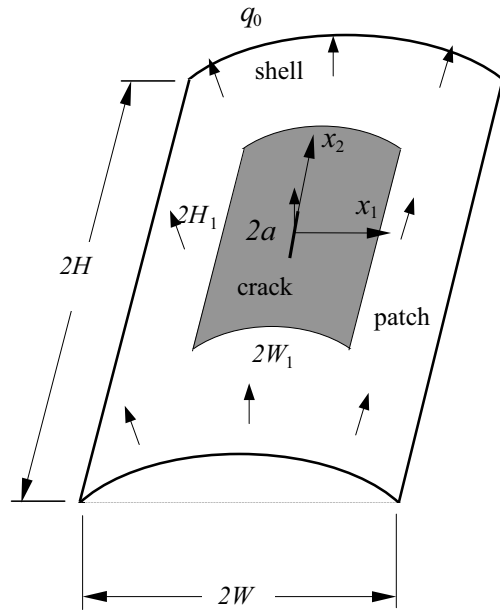
It is clear that the maximum and minimum values of stress intensity factors K_I and K_{II} occur on either the upper surface of the sheet or the lower surface and K_{III} occurs on the mid-plane of the sheet. To obtain more accurate solutions of the displacement in the crack front, special elements [Dirgantara, Aliabadi (1999)] are used.

5 Numerical examples

Example 1. Clamped rectangular cylindrical shell with patch

A rectangular cylindrical clamped shell subjected to uniform pressure q_0 as shown in Figure 4 is analysed. The material constants for the shell and the patch are the same, with Young's modulus $E = 210$ GPa and Poisson's ratio $\nu = 0.3$. The shell is of dimensions $-6p \leq x_1 \leq 6p$, $-9p \leq x_2 \leq 9p$ and thickness $h_0 = 1.6$ mm, where p is the pitch of rivet and is chosen as 25.4 mm. The diameter of the rivet is $\phi = 4$ mm and thickness $h_1 = h_0$. Curvatures $k_{11} = 1/60p$, $k_{22} = 0$ and the uniform load $q_0 = 1$ MPa. All four sides of the cylindrical shell are clamped, that is $u_\alpha = w_i = 0$ on all boundaries.

The boundaries of the shell and patch are divided into 24 and 20 continuous quadrature elements respectively; 98



- Boundary nodes
- DRM points
- Rivet position

Figure 4 : Patched rectangular segment of a cylindrical shell and BEM mesh with distribution of domain point.

domain points including 54 rivet points are used and the distribution of domain points is shown in Figure 4. The numerical results for deflections, moments and membrane forces of shell along x_2 are plotted in Figures 5-7. The results for the patched and non-patched cases is also shown in these figures. A reduction of deflection and internal forces can also be seen. Comparisons have also been made with the finite element method for deflection, moment and membrane forces. Excellent agreement is achieved.

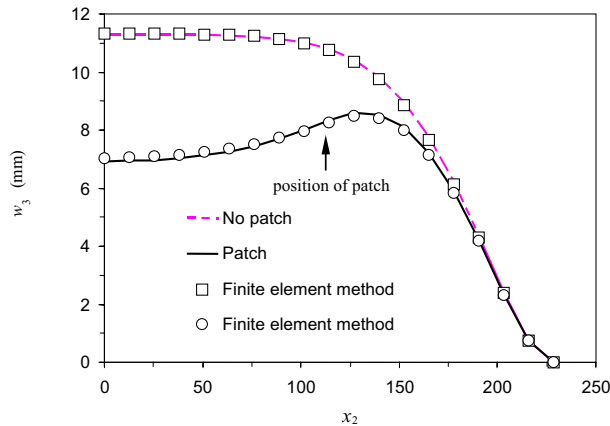


Figure 5 : Deflection along the x_2 axis (mm).

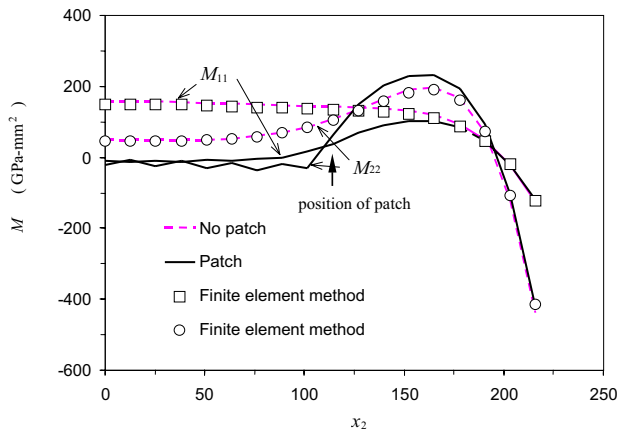


Figure 6 : Distribution of moments along the x_2 axis.

Example 2. Centrally cracked cylindrical shell with circular patch

Consider a centrally cracked rectangular cylindrical shell ($k_{11} = 0, k_{22} \neq 0$), as shown in Figure 8, subjected to either a moment load or a membrane load at two ends of the shell. The simply supported boundary condition is

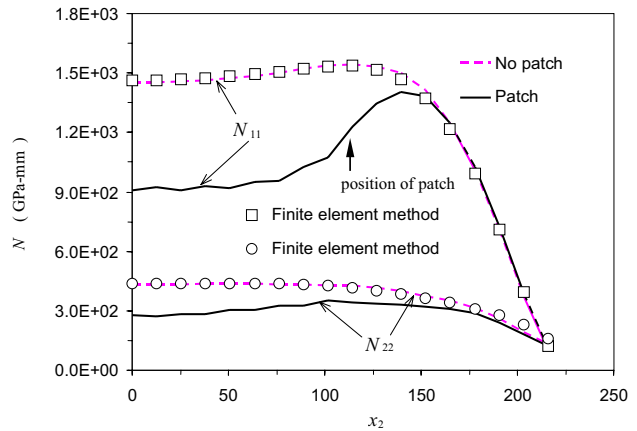


Figure 7 : Membrane forces along the x_2 axis.

applied only to the top and bottom sides of the sheet and the other two sides are traction free. The boundary conditions for the cylindrical shell are defined as

$$p_1 = p_2 = w_3 = 0, \quad t_2 = \sigma_0 \quad \text{on } x_2 = \pm W$$

and the traction free condition for all the other boundaries of the shell and on the boundary of circular patch. The geometries are: width of the shell $2W (= 2 \times 90\text{mm})$, the circular patch radius $R = 30\text{ mm}$ and thickness $h = h_1 = 1.5\text{ mm}$; material constants: $E = E_1 = 70\text{ GPa}$, $\nu = \nu_1 = 0.3$. The boundary element meshes (48 elements are used for shell boundary including the crack surfaces, 32 element on the circular patch, and 94 domain points including 18 rivet points in the patch area) and the rivet distribution are shown in Figure 8. The numerical results of the maximum normalized stress intensity factors K_I^{max} on the bottom of the patched shell under a moment load M_0 and membrane load N_0 on the ends are plotted against the curvature of the shell in Figures 9 and 10 respectively for different crack lengths. Because of the patch, the normalized stress intensity factors decrease for longer cracks. It is interesting to note that the stress intensity factors for different crack lengths are almost the same and have a linear relation with curvature k_{22} . By changing the value of the patch thickness h_1 , the curves of the maximum stress intensity factors against the curvature of shell due to moment load and membrane load at two ends are plotted in Figures 9 and 10 .

6 Conclusion

A boundary element method coupled with the two-dimensional stress plane problem and bending problem

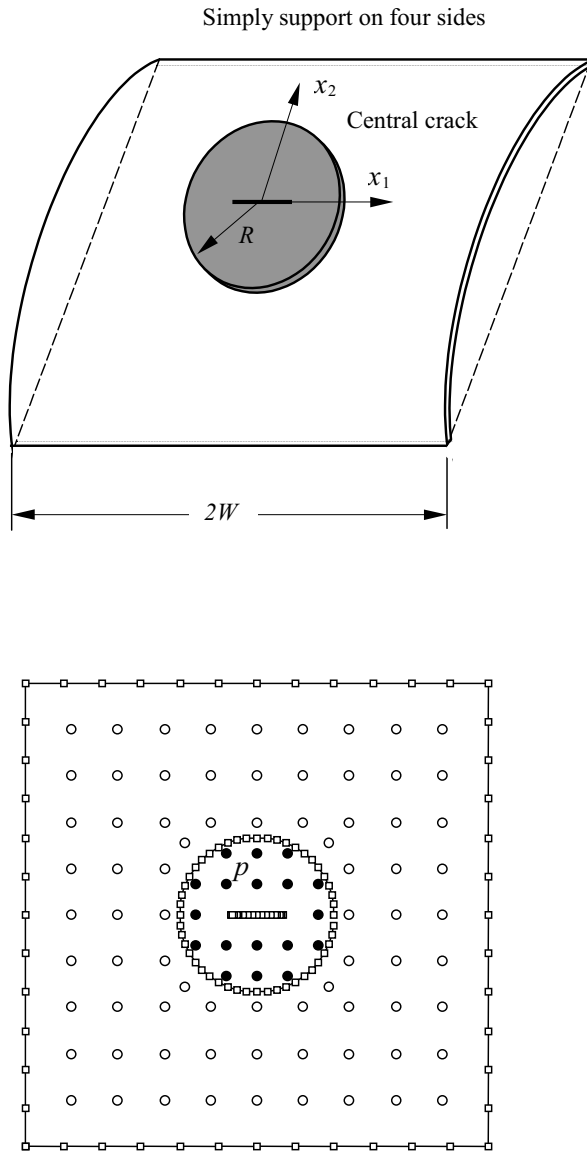


Figure 8 : Cracked square segment of a cylindrical shell with a circular patch and BEM mesh.

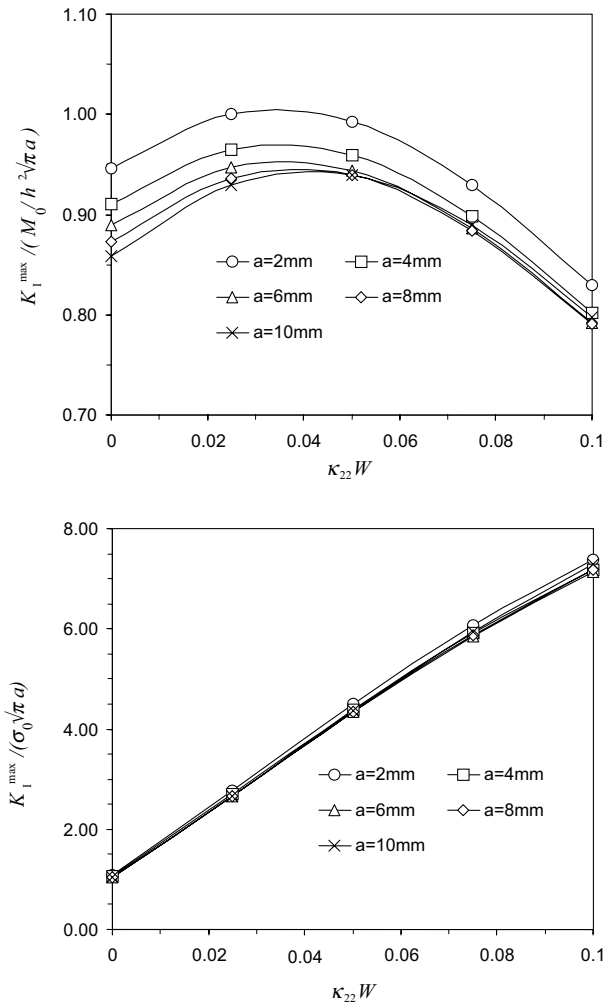


Figure 9 : Normalized maximum stress intensity factors due to moment load M_0 and tension load N_0 varied with curvature k_{22} and crack length a .

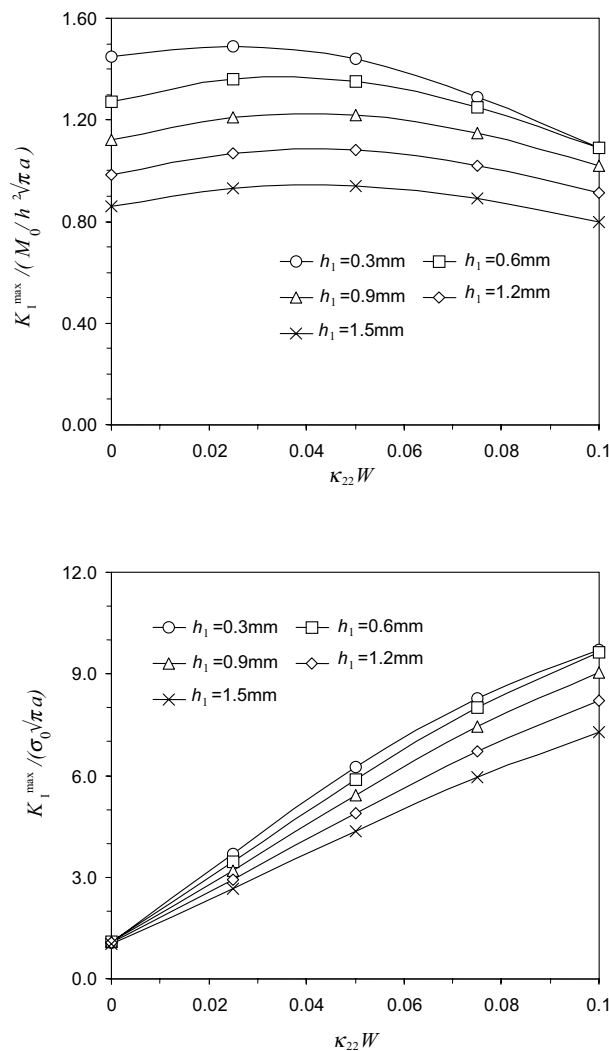


Figure 10: Normalised maximum stress intensity factors due to moment load M_0 and tension load N_0 varied with curvature k_{22} and thickness of patch h_1 .

has been developed for the analysis of cracked curved panels with a rivet repair. Domain integrals occurring in the boundary integral equations are transformed to boundary integrals using the dual reciprocity method. The effect of the rivet patches is replaced by distributional forces on the cross-section of the rivets. It was shown that the dual boundary element method is an effective method to deal with cracked curved panels repaired with mechanically fastened patches.

Acknowledgement: This work has been carried out with the support of the Ministry of Defence, Defence

Evaluation and Research Agency, FARNBOROUGH, Hants, U.K.

References

- Chu, R. C. and Lin, Y. S.** (1993): Bulging of cracked panel in extension due to unbalanced patching, *Theor. Appl. Fract. Mech.*, Vol.19, pp. 13–27.
- Park, J. H., Ogiso, H. and Atluri, S. N.** (1992): Analysis of Cracks in Aging Aircraft Structures, with and without Composite-Patch Repairs, *Computational Mechanics*, Vol. 10, pp. 169-201.
- Chow, W. T. and Atluri, S. N.** (1997): Composite Patch Repairs of Metal Structures: Adhesive Nonlinearity, Thermal Cycling and Debonding, *AIAA Journal*, Vol. 35(9), pp. 1528-1535.
- Fawaz, S. A.** (1997): *Fatigue Crack Growth in Riveted Joints*, Delft University Press, The Netherlands.
- Aliabadi, M. H.** (1998): *Plate Bending Analysis with Boundary Elements*, Computational Mechanics Publications, Southampton.
- Salgado, N. K. and Aliabadi, M. H.** (1997): The analysis of mechanically fastened repairs and lap joints, *Fatigue Fract. Eng. Mater. Struct.* Vol. 20, pp. 583-593.
- Sih, G. C. and Hagendorf, H. C.** (1997): On cracks in shells with shear deformation, *Mechanics of Fracture*, edited by Sih, G. C., Vol. 3, pp. 201–229.
- Wen, P. H., Aliabadi, M. H. and Young, A.** (1999): Transformation of domain integrals to boundary integrals in BEM analysis of shear deformable plate bending problems, *Computational Mech.*, Vol. 23(4), pp. 304–309.
- Wen, P. H., Aliabadi, M. H. and Young, A.** (2000): Plane stress and plate bending coupling in BEM analysis of shallow shells, *Int. J. Num. Meth. in Engng*, Vol. 48, pp.1107–1125.
- Vander Weeën, F.** (1982): Application of the boundary integral equation method to Reissner's plate model, *Int. J. Numer. Methods Engng*, Vol.18, pp.1–10.
- Dirgantara, T. and Aliabadi, M. H.** (1999): A new boundary element formulation for shear deformable shells analysis, *Int. J. Num. Meth. in Engng*, Vol. 45, pp. 1257–1275.
- Swift, T.** (1974): The effects of fastener flexibility and stiffener geometry on the stress intensity in stiffened cracked sheets, *Proc. Conf. on Prospects of Fracture Mechanics, Delft*, pp. 419–457.